Zentrum für Technomathematik
Fachbereich 3 – Mathematik und Informatik

Simulation-based Multiobjective Optimization for Milling Processes

Jonathan Montalvo-Urquizo
Carsten Niebuhr
María G. Villarreal-Marroquín

Report 17–02

Berichte aus der Technomathematik
Report 17–02 Februar 2017

SIMULATION-BASED MULTIOBJECTIVE OPTIMIZATION FOR MILLING PROCESSES

JONATHAN MONTALVO-URQUIZO, CARSTEN NIEBUHR, AND MARÍA G. VILLARREAL-MARROQUÍN

Abstract. This paper presents the optimization of a dry machining process, where thermo-mechanical effects, like shape deviations, and a time dependent domain are major challenges. First, the simulation model to compute finite element approximations to a general milling process is presented. The model includes a submodel (dexel model) for material removal and process forces and heat flux introduced by the machining tool. In a second part, we present an optimization algorithm based in metamodels that serve as a tool to improve processes with different performance measures that exhibit conflicting behavior. With this metamodel-based optimization we avoid the use of a large number of high-fidelity computer simulations, which are commonly expensive.

The approach is tested on two case studies for optimizing (a) workpiece deformation and equivalent stress after milling, and (b) equivalent stress and milling process time.

1. Introduction

For manufacturing businesses to be successful in the global market, they must strive to deliver high quality products at the lowest possible cost. One approach to select the processing conditions to achieve these goals is to run experiments on the manufacturing floor. Such experimentation is usually costly and requires considerable amount of time and effort, which may not be feasible during production [5]. Alternatively, advanced computer simulations can be used to represent the processes. Such computer simulations along side with optimization methods are used to identify the values of the controllable processing variables that optimize the relevant performance measures (PMs). In this work, we present an integrated framework to find optimal process parameters for a milling operation using a combination of metaheuristic optimization models and thermomechanical finite element (FEM) simulations.

Milling of metallic components is a machining operation based on the removal of material using a multi-edged rotating tool and a relative motion of the tool and the component that generates the so-called feed of the milling process, [15, 17]. Commonly, the feed and turning

velocities of the machining process are operated using a Computer Numerical Control (CNC) system on what is called NC machining centers. The resulting geometry of the milled component is determined by the feed trajectory of the machining process, removing a chip of material in each pass of the cutting insert, [2–4]. The left draw on Figure 1.1 illustrates a milling rotating tool and its main parameters.

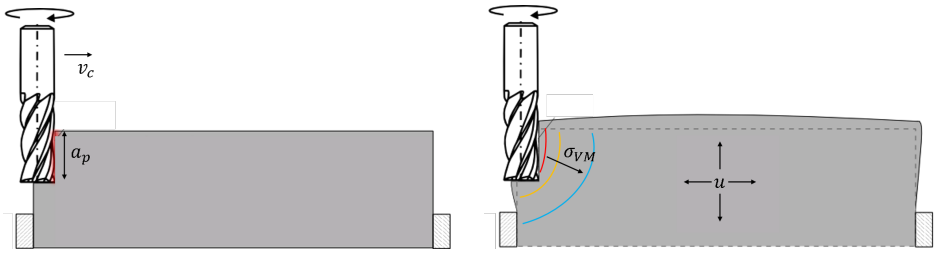

FIGURE 1.1. *Left:* Milling rotating tool and its main parameters illustrated over the original geometry of the component. *Right:* Illustration of thermomechanical effects on the component resulting in thermal expansion and stress

It is well known that the cutting of material chips and friction of the cutting tool with the component produces heat. In some cases, the reached temperatures may lead to non-controlled material deformation and results in undesired deflections on the machined product. The drawing on the right side of Figure 1.1 shows the thermomechanical deformation effect of a milled part. Then, there is big interest on generating simulative tools to better understand the thermal effects arising during the milling process.

In this sense, a thermomechanical simulation in which the temperature generated is used as input to simulate the thermal expansion and the corresponding mechanical deformation of the components is needed, [2]. In this work, we consider Adaptive FEM simulations implemented in ALBERTA [13] which share the coupled thermomechanical spirit of previous works on heat treatment [16], laser welding [8], and forming [9].

Joining simulation and optimization for defining the best possible process parameters is an actual need in current engineering practice [19, 21, 22]. This often comes together with the issue of evaluating an optimization functional that request to run a complete simulation which is computationally expensive at every candidate solution [6]. As for many other real processes, the milling simulation can require a large amount of computations and, in dependence of the process complexity, a single simulation evaluation can take minutes to even days.

For this type of problems, optimization methodologies for simulation outputs are typically based on surrogate models (or metamodels)

which are mathematical models that try to mimic the behavior of the simulation model based on a limited number of observations [1, 7, 21]. Metamodels help reduce the computational effort required to evaluate the performance measures at different process conditions, as they are faster to evaluate than the simulation model. Surrogate models are also convenient for cases when it is only possible to use experimental data and a single process evaluation is expensive and time consuming. Therefore, by utilizing surrogate models it is possible to use an optimization technique that requires the evaluation of the process at a high number of processing conditions. The most commonly used surrogate models are Response Surface, Kriging, Radial Basis Function (RBF), and Artificial Neural Networks. Reviews of surrogate models used in optimization via simulation can be found in [1, 7, 14, 21].

In the following sections, the milling process and its thermomechanical simulation (Section 2), the metamodel-based optimization method (Section 3), and two case studies where simulation and optimization are merged to obtain the set of optimal PMs (Section 4) are presented. Finally, we present some conclusive remarks in Section 5.

2. Numerical process simulation

We use an Adaptive FEM simulation for the milling process considering the connection of a dexel model and the thermal and mechanical equations as presented in [2]. The models consist of an extension of a classical NC-Simulation to emulate thermomechanical effects making a difference between the model for the workpiece and the process model (see Figure 2.1).

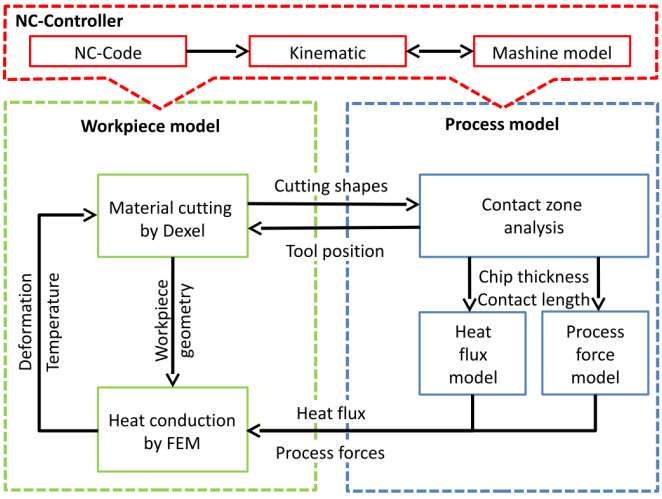

Figure 2.1. Detailed information flow of simulation system

The workpiece model describes the current state of the workpiece in geometrical and thermomechanical aspects (Figure 2.1 left). A material removal simulation via a dexel model allows to represent the change of the geometrical representation during the process. A FE-model calculates temperature and linear deformation to represent the thermomechanical workpiece behavior.

The process model has several calculation steps (Figure 2.1, right). The cutting conditions are calculated from the geometrical intersection of the tool and the workpiece. With this data, the cutting force and heat flux are predicted and the mechanical and thermal loads are calculated. This changes the boundary conditions of the FE-model. The shape deviations generated by the material cutting process are predicted based on the calculated temperature and deformation behavior of the workpiece. For detailed descriptions of these calculations see [2–4, 10].

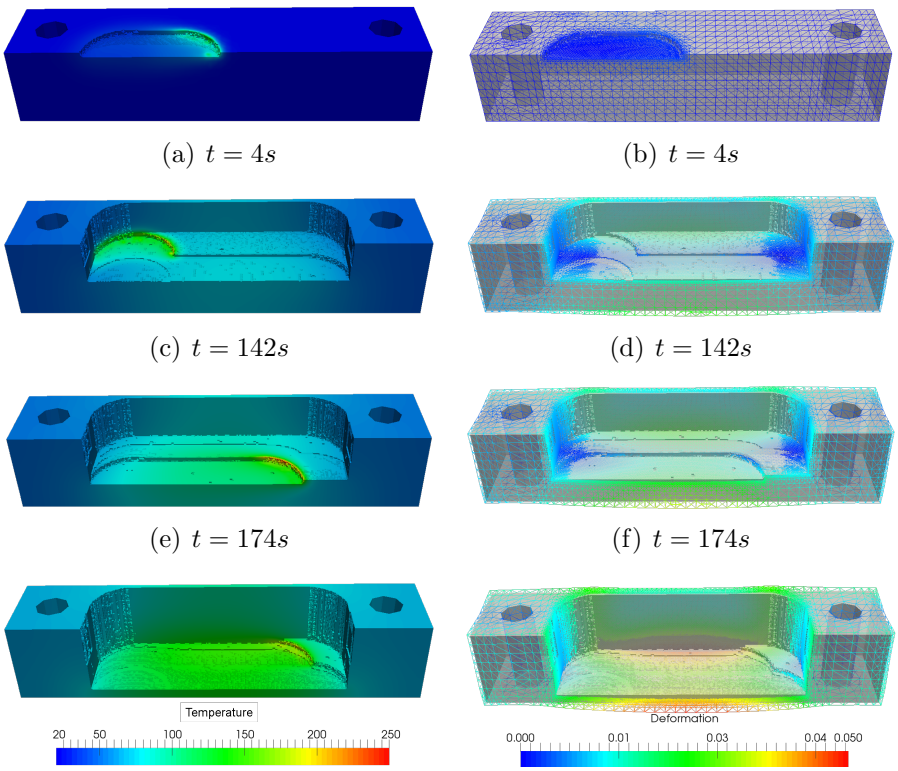

(a) $t = 4s$ (b) $t = 4s$

(c) $t = 142s$ (d) $t = 142s$

(e) $t = 174s$ (f) $t = 174s$

(g) $t = 240s$ (h) $t = 240s$

FIGURE 2.2. Simulation of milling at different process times. *Left:* Temperature, *Right:* Deformation using a scaling factor of 100

2.1. **Simulation of milling processes.** Now we present the simulated milling process and some FEM simulation results that serve to

determine a reduced geometry to be used to estimate the performance measures values for the optimization in Section 3.

2.1.1. *Reference process.* The machining of a thin walled part made of 1.1191 Steel has been chosen as reference process and it has been used in different works, [3,4,10]. The blank part is a rectangular workpiece 40mm width, 40mm thick and 195mm of length. The percentage machined material is about 60% (see Figure 2.2). The workpiece is clamped on two sides, with one degree of freedom for torsion and translation. The sides are fixed on a dynamometer, which allows to measure the fixture forces. The machining strategy is z-level constant, the roughing process is divided in different steps for every level and a finishing step of the thin wall is performed in one cut and with different number of levels, [4].

2.1.2. *Simulation results.* The mathematical model to simulate the thermomechanical behavior of the workpiece during the machining process has been presented in [10]. It includes the description of the heat equation and the quasi-stationary linear elasticity equation on a time-dependent domain with boundaries changing in every time step. This coupled system is implemented using the Adapted Finite Element Toolbox ALBERTA [13].

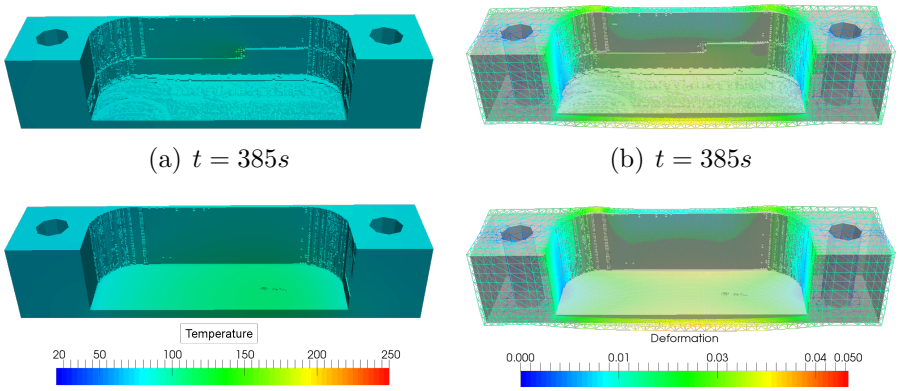

(a) $t = 385s$ (b) $t = 385s$

(c) $t = 507s$ (last timestep) (d) $t = 507s$ (last timestep)

FIGURE 2.3. Simulation of milling during finishing and at the process' end. *Left:* Temperature, *Right:* Deformation using a scaling factor of 100

The milling process is divided into two parts, a roughing and a finishing part. Roughing is the removal of large portions of material out of the workpiece, while the finishing step is a detailed material removal of only few μm and it is performed at the end.

Figures 2.2 and 2.3 show the simulation results for temperature and mechanical deformation at some fixed times. The roughing is shown in

Figure 2.2 and the finishing step in Figure 2.3 (a)-(b). Finally, Figure 2.3 (c)-(d) show the simulated workpiece at the end of the process.

The simulation results have shown to be in accordance with experimental data for both temperature and deformation [4]. The thermomechanical implementation has also been used to simulate more detailed milling processes with thin walled workpieces for lightweight structures.

2.2. **Simulation setting for optimization.** In practice, when the produced workpieces present geometric deviations above the allowed tolerances, a costly correction step is needed, and it might even be necessary to adjust the process parameters, [11,12]. In order to improve the results of a milling process, we intend to connect the simulation model with an optimization procedure.

For this, we consider some input parameters like the cutting width a_e, cutting depth a_p, cutting velocity v_c, feed rate v_f, among others. Different process parameter will result in different material removal conditions which change the shape of the current workpiece Ω_t. As process output, we consider the geometric change in the domain Ω_t as well as the effects on thermal expansion on the face where the cut is done. These thermomechanical undesired effects can be observed by measuring the resulting deformation and stress.

Additionally, in order to maintain the simulation affordable, we reduced the analyzed workpiece to a subdomain of the complete geometry defined as a slice 5mm thick located in the longitudinal center of the workpiece, as illustrated in Figure 2.4. The slice is an L-shaped geometry after the milling process is performed. Within this small domain we want to find the optimal process parameters to obtain the smallest deformation and stress.

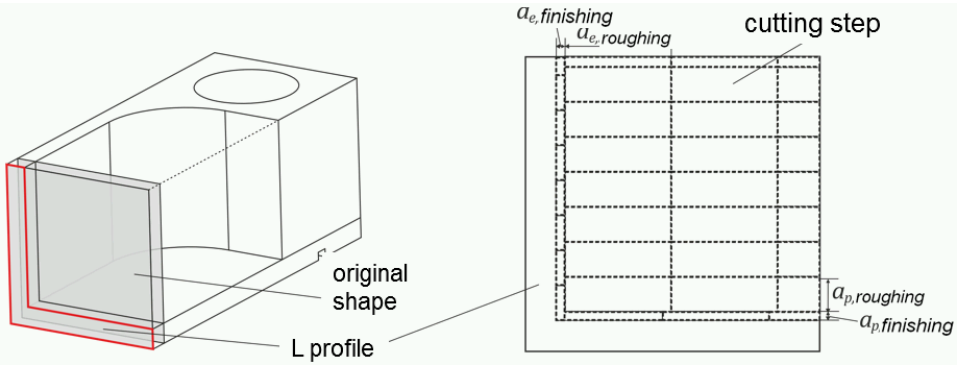

FIGURE 2.4. Model process for optimization, L-shaped domain

3. MULTIOBJECTIVE OPTIMIZATION METHOD

Real manufacturing problems often involve different PMs that exhibit conflicting behavior. For example, the processing conditions that

provide the best quality product may not correspond to the lowest production cost. Such situations are strongly present in the milling process that was presented in Section 2. For this reason, we are interested in a methodology to get improvements of a generalized form of performance where several criteria can be studied together.

When multiple conflicting PMs are involved, optimizing a single objective can result in solutions that perform poorly for other objectives. Thus, it is not the best approach to obtain a single solution but rather the set of solutions corresponding to the best compromises. For this, we use the following definition of Pareto solutions:

3.1. **Definition.** A feasible solution $\mathbf{x}_1$ of the optimization problem minimize $(f_1(\mathbf{x}), f_2(\mathbf{x}), \ldots, f_m(\mathbf{x}))$ is said to dominate $\mathbf{x}_2$ if: $f_i(\mathbf{x}_1) \leq f_i(\mathbf{x}_2)$ $for\, i = 1, \ldots, m,$ and $f_i(\mathbf{x}_1) < f_i(\mathbf{x}_2)$ for some $i \in \{1, \ldots, m\}$. The non-dominated solutions are known as *Pareto solutions*. The set of Pareto solutions is known as *Pareto Set* (P_{set}) and the corresponding output values form the so called *Pareto Front* (P_{front}).

Given a problem with conflicting PMs, we can focus our attention on finding the Pareto set, and then a decision maker can select the best one on a particular moment of the process. This allows for the decision maker to give different importance to the PMs at any time, once the set of non-dominated solutions is known.

In this work, we use an adapted version of the metamodel-based multiobjective simulation optimization method introduced in [18] to optimize two case studies for a milling process.

The method is schematically shown on Figure 3.1 and starts by performing an experimental design to collect a set of initial data points, and a simulation run is performed at each point. Then the set of best compromises between all performance measures is found using Definition 3.1, and it is called *Incumbent Pareto Front*. Using this, the main iteration steps are the following:

(1) Use all available simulated data to fit a metamodel for each PM.
(2) Use the metamodels to estimate the value of the PMs for a large set of input combinations.
(3) Identify the best compromises between all PMs. Call the corresponding Pareto Front, *Predicted Pareto Front*. The corresponding controllable variables settings are the *predicted Pareto Set* ($\tilde{P}_{set}$).
(4) Evaluate the predicted Pareto Set using the simulation code.
(5) Update the incumbent Pareto Front (based on simulated data) using the new information.
(6) Evaluate stopping criteria.

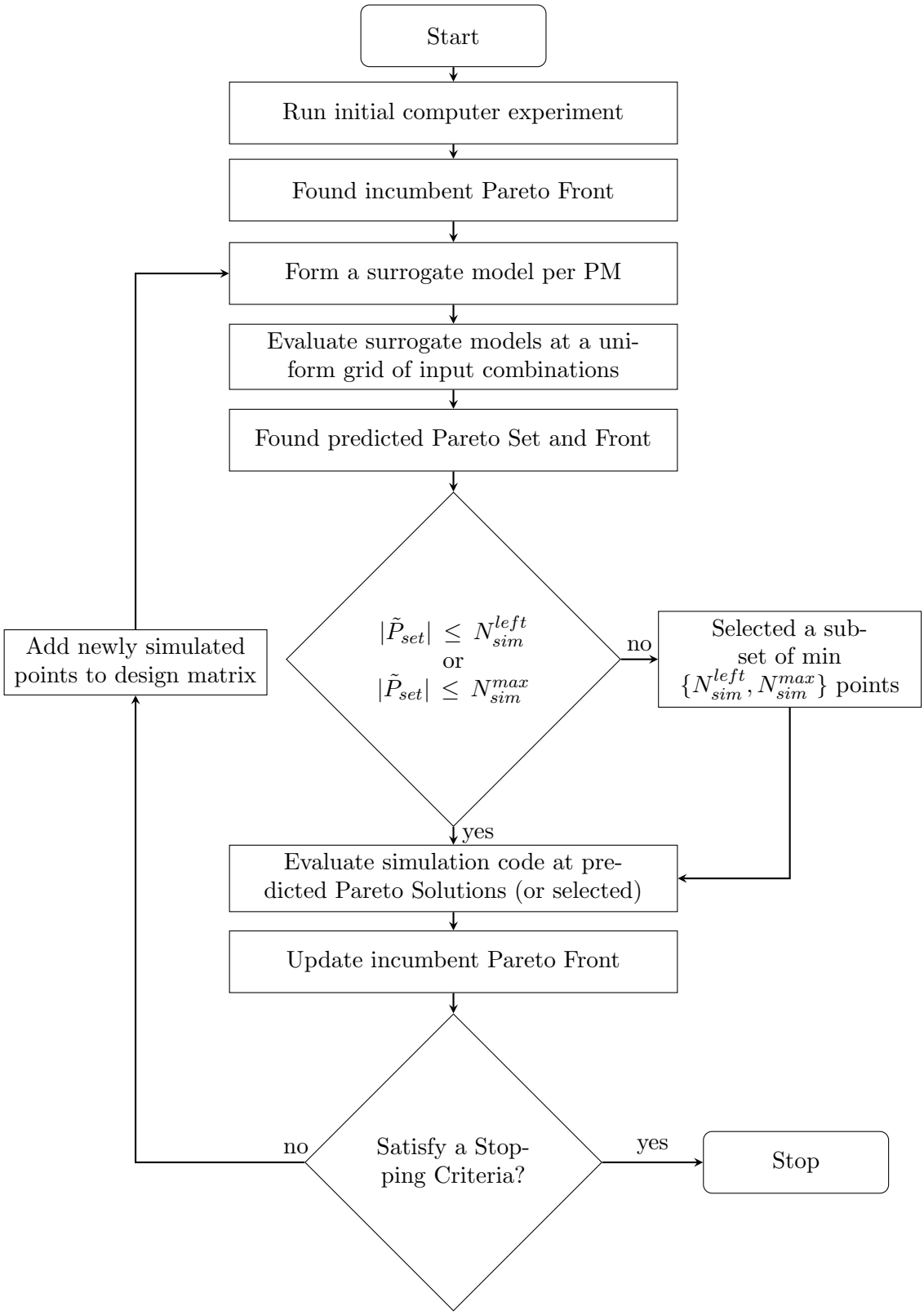

FIGURE 3.1. Multiobjective optimization method flow diagram

It is important to mention that at step 4, if the number of solutions on the predicted Pareto Set is larger than the remaining number of simulation runs allowed (N_{sim}^{left}), or it is larger than the maximum number of simulations allowed per iteration (N_{sim}^{max}), a subset of $\min\{N_{sim}^{left}, N_{sim}^{max}\}$ solutions is selected based on a Maximin distance criterion using the predicted Pareto Front. A value of $5n$, where n is the number of controllable variables, is recommended for N_{sim}^{max}.

Using these iterative steps, the metamodels are updated and are used to approximate a new Pareto Set. The updated models are able to obtain good approximations of the output responses near the Pareto Front at each iteration.

At each iteration a series of stopping criteria are evaluated and if at least one is met, the method stops and reports the incumbent Pareto Solutions, otherwise, the new simulated points are added to the existing set of data points and a new iteration begins. The stopping criteria we used in this implementation are:

- Stop if the total number of simulation (N_{sim}^{total}) allowed is reached
- Stop if the coefficient of determination R^2 of all models is larger than $1 - \varepsilon$
- Stop if no new Pareto solutions are found

It has been demonstrated in [18] that this multiobjective optimization method is able to approximate a set of Pareto solutions without having to evaluate a large number of simulations. $15n$ has been shown to be a good upper limit for the total number of simulations (N_{sim}^{total}). In [20], the method was used to solve two case studying on an injection molding process. The results were compared with an approach based on Gaussian process metamodels and it was shown that both methods perform comparably.

4. Case Studies

In machining operations, the produced heat results in thermomechanical distortion of the workpiece and thereby in incorrect material removal by the cutting tool. Especially in machining thin walled parts for lightweight structures, an additional finishing step is needed if the resulting shape deviations are large. In this context, the aim for mathematical optimization of a milling process is to minimize the resulting distortion in the produced workpiece.

In this Section, we present two optimization case studies of a milling process with two process' PMs simultaneously.

4.1. **Case Study 1: Deformation and stress.**

The optimization on this case study has two PMs and two process controllable variables. The considered optimization goals are minimize *deformation* (u) and minimize *equivalent stress* (σ_{vM}). As process controllable variables we considered *cutting velocity* (v_c) and *axial cutting depth* (a_p). The ranges

used for the controllable variables are [100, 300] (m/min) and [5, 30] (mm) for v_c and a_p, respectively.

The rest of the process variables are considered as fixed considering the values as the ones listed in Table 1. Other typically considered variables (like spindle speed, feed speed and feed per revolution) can be calculated from the value of the cutting velocity v_c and the values in Table 1.

Variable	Value	
Radial depth of cut	$a_e = 20$	[mm]
Number of teeth	$z = 4$	[-]
Feed rate per tooth	$f_z = 0.20$	[mm/tooth]
Cutter diameter	$D = 40$	[mm]
Average chip thickness	$h_m = 0.20$	[mm]

TABLE 1. Process simulation setting values of fixed variables for Case Study 1 and 2

Deformation u is calculated as the average of the Euclidean Norm of 3 given points on the outer side of the thin wall near the inner corner of the final workpiece and stress is given as the volume average of the Von Mises stress σ_{VM} in a cylinder with radius $1mm$ around the inner corner point of the final workpiece.

The process simulations are running on a workstation with four CPUs (Intel i7-3770, 3.4 GHz) by using one CPU for the finite element simulation and one CPU for the material removal. All processes start with 242 degrees of freedom (DOFs), 600 active elements inside and zero non-active elements outside the workpiece. During the process the number of DOFs and elements decrease by the adaptive approximation of the geometry change in average up to 22 000 DOFs, 95 800 non-active elements outside and 17 800 active elements inside the final workpiece. The simulation time and timesteps depends on the varying v_c and a_p.

For the multiobjective optimization algorithm we used the following parameters: as suggested in [18], the maximum number of evaluations allowed was set to $N_{sim}^{total} = 30$; the maximum number of runs per iteration was set as $N_{sim}^{max} = 10$; and the lower bound for R^2 was set at 99% ($\varepsilon = 0.01$).

The optimization procedure is as follows:

Initialization

(1) *Run initial experimental design*
The first step of the method is to design and run an experiment to get an initial sample of data points: as suggested in [20] a Central Composite Design is used. The values of the controllable variables and corresponding performance measures are

Run	v_c [m/min]	a_p [mm]	σ_{vM} [MPa]	$\|u\|_2$ [mm]	Proc. time [min]
1	100.00	17.50	477.29	0.0709	4.97
2	129.29	8.66	562.30	0.1102	7.13
3	129.29	26.34	346.23	0.0357	2.75
4	200.00	5.00	300.25	0.1085	6.73
5	200.00	17.50	296.99	0.0334	2.48
6	200.00	30.00	249.59	0.0252	1.80
7	270.71	8.66	353.52	0.0460	3.41
8	270.71	26.34	215.12	0.0228	1.32
9	300.00	17.50	219.31	0.0243	1.66

TABLE 2. Results of initial experimental design

shown on Table 2. Figures 4.1 and 4.2 show in black dotes (1 to 9) the controllable variables and PMs values, respectively.

(2) *Find incumbent Pareto Front*
After all data has been collected, the incumbent Pareto Front is identified. The incumbent Pareto solutions, from the initial points, is solution 8 (see Figure 4.2).

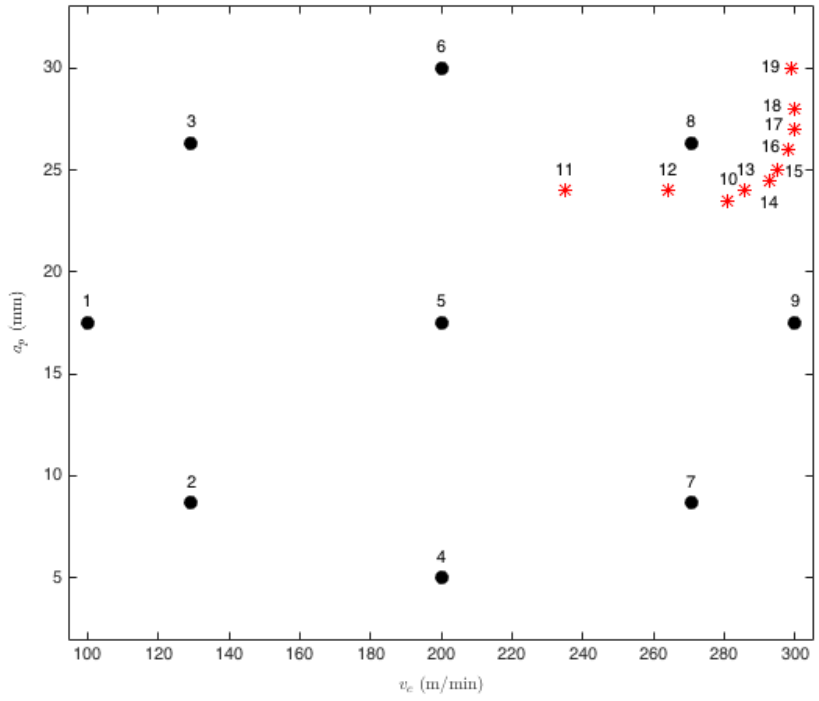

FIGURE 4.1. Case Study 1: Controllable process variables values of initial experiment (black dotes, $\{1, 2, \ldots, 9\}$) and extra runs (stars, $\{10, 11, \ldots, 19\}$)

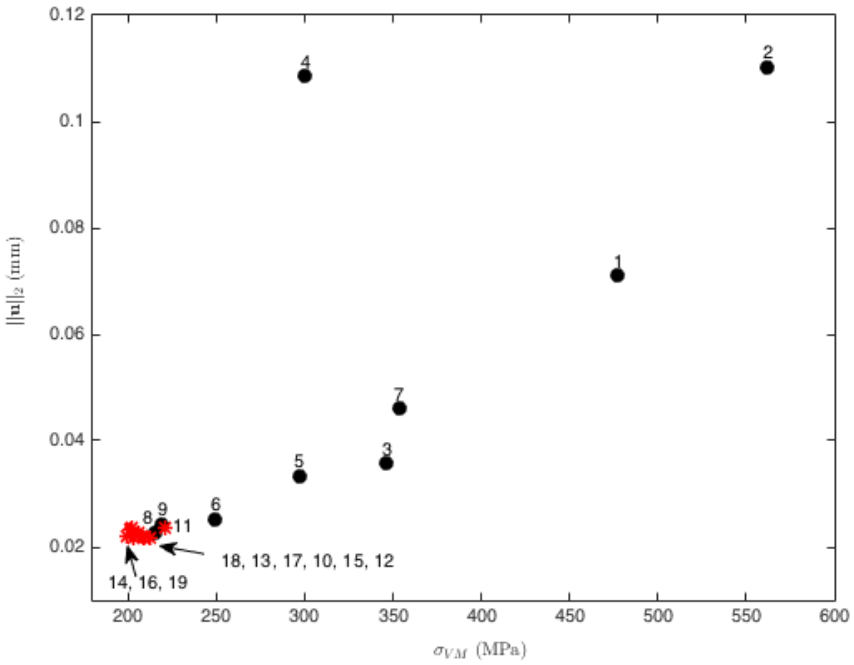

FIGURE 4.2. Case Study 1: PMs values of initial experiment (black dotes, $\{1, 2, \ldots, 9\}$) and extra runs (stars, $\{10, 11, \ldots, 19\}$)

Main Iteration

(1) *Form a surrogate model per performance measure*
A surrogate model is fitted for each PM using all available experimental data. The fitted models used here are Multiple Linear Regression (MLR) models with one degree of freedom. The coefficients of determination R^2 of the surrogate models are $R_1^2 = 0.9395$ (stress) and $R_2^2 = 0.9974$ (deformation).

(2) *Evaluate surrogate models at a uniform grid of input combinations*
The surrogate models are evaluated at a uniform grid of 201x51 input combinations. Figure 4.3 shows the evaluation of the models; where, $\hat{f}_1$ estimates (interpolates) stress and $\hat{f}_2$ estimates deformation.

(3) *Found approximated Pareto Set and Front*
Now, the Pareto Front of the predicted solutions is found. The predicted Pareto Front has 118 solutions. However, since the maximum number of simulations allowed per iteration $N_{sim}^{max} = 10$, 10 solutions were selected using a max-min distance criteria algorithm with 1000 iterations. This is, 1000 subsets of 10 points were randomly selected out of the 118 points and the set

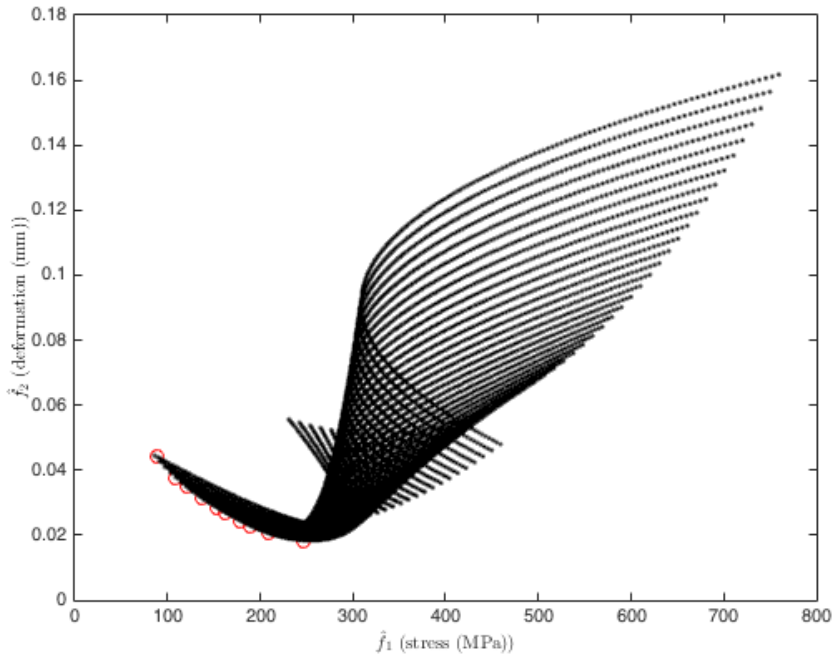

FIGURE 4.3. Case Study 1: (a) Predictions of meta-models with selected predicted Pareto Solutions (circled solutions)

which minimum distance between two points is the maximal was selected. The circled solutions on Figure 4.3 are the 10 selected predicted Pareto solutions.

(4) *Evaluate selected predicted Pareto Solutions*
Table 3 shows the input and output values of the 10 new runs. Figures 4.1 and 4.2 show the results graphically as red stars (solutions 10 to 19). The simulations were carried out using the same fixed parameters as the initial runs.

(5) *Update Incumbent Pareto Front*
The Incumbent Pareto Front is updated comparing the initial incumbent Pareto Front (solution 8) and the 10 new additional runs. The new Pareto solutions are 12 and 14.

(6) *Evaluate Stopping Criteria*
Next the stopping criteria are evaluated. The criteria used here are: (1) stop if the maximum number of simulation allowed was reached (no, $19 < 30$); (2) stop if R^2 of all models is larger than $1 - \varepsilon = 0.9900$ (no, $R_1^2 = 0.9395$ and $R_2^2 = 0.9974$); (3) stop if no new Pareto solutions were found (no, new solutions were

Run	v_c [m/min]	a_p [mm]	σ_{vM} [MPa]	$\|u\|_2$ [mm]
10	281.00	23.50	207.35	0.0221
11	235.00	24.00	221.27	0.0236
12	264.00	24.00	212.13	0.0218
13	286.00	24.00	203.56	0.0223
14	293.00	24.50	199.60	0.0219
15	295.00	25.00	208.83	0.0219
16	298.00	26.00	201.57	0.0232
17	300.00	27.00	205.51	0.0227
18	300.00	28.00	203.35	0.0219
19	299.00	30.00	201.92	0.0236

TABLE 3. Case Study 1: Evaluation of selected predicted Pareto solutions

Run	v_c [m/min]	a_p [mm]	σ_{vM} [MPa]	$\|u\|_2$ [mm]
12	264.00	24.00	212.13	0.0218
14	293.00	24.50	199.60	0.0219

TABLE 4. Case Study 1: Final Pareto Solutions

found). Since none of the stopping criteria were met, a new (main) iteration begins.

Second iterations
On the second iteration, new metamodels were fitted using all available data (19 simulations). The R^2 of the new models are $R_1^2 = 0.9997$ and $R_2^2 = 0.9999$. Later, the models were used to predict a new Pareto front which only has one new solution, $\mathbf{x_{20}} = (100, 30)$. Then, a simulation run was performed using $\mathbf{x_{20}}$ and the corresponding outputs are $\mathbf{f_{20}} = (394.08, 0.0482)$. Afterwards, the incumbent Pareto front was update but did not changed. Then, the stopping criteria were evaluated and since the R^2 of both models are larger than 0.99 the method stopped and the final Pareto solutions are reported.

Report Final Incumbent Solutions
The final Pareto solutions are shown on Table 4. From this table it can be noticed that both solutions have similar performance and the axial depth is similar too. However, solution 12 requires a slower cutting velocity than solution 14 but it generates higher stress. In a practical application, the specific component production will always include some extra information given by the decision maker and is in this form that we are able to select one Pareto solution and dismiss the others.

4.2. **Case Study 2: Time efficiency and stress.** To further investigate the optimization of the milling process, now we consider the time spent to perform one complete milling process together with the resulting workpiece stress.

As in Case Study 1, the optimization was conducted following the flow chart in Figure 3.1, using the same controllable variables and process parameters. The initial design of experiments is the same Central Composite Design as Case Study 1. For this input values, Table 2 shows the values of the PMs: stress and processing time. The PMs values are also shown graphically on Figure 4.4 as black dotes. The initial Pareto solution is solution 8.

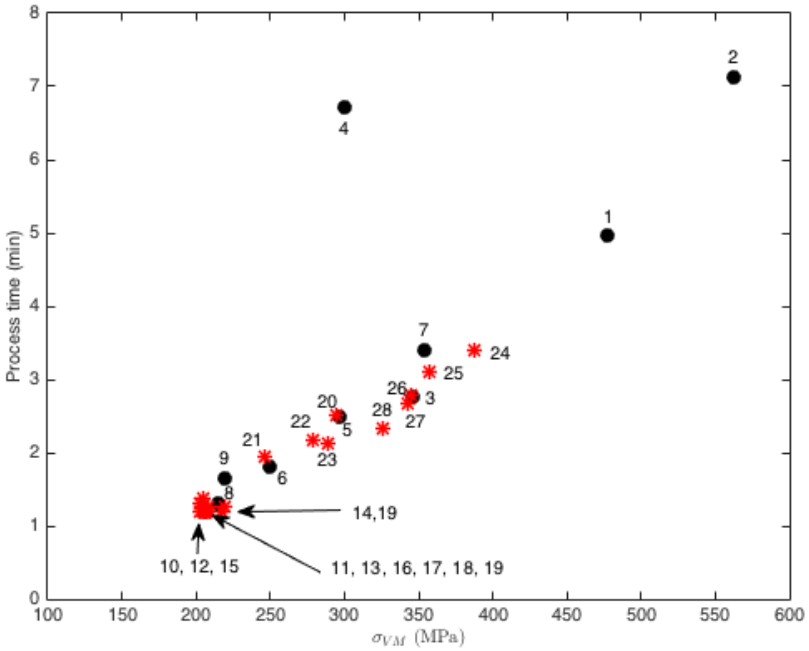

FIGURE 4.4. Case Study 2: PMs values of initial experiment (black dots, $\{1, 2, \ldots, 9\}$) and extra runs (red stars: 10 to 19 (iteration 1) and 20 to 29 (iteration 2)

Then, saturated MLR models were fitted to estimate stress and process time. The R^2 of the metamodel for stress is 0.9395 and 0.9990 for process time. The performance measures values of 10,251 (201 x 51) solutions were calculated and the predicted Pareto Front identified. The predicted Pareto Front has 101 solutions but only 10 were selected and simulated. Table 5 shows the results of the 10 additional runs (solutions 10 to 19).

Now the incumbent Pareto Front is updated comparing the initial Pareto Front (solution 8) and the additional 10 simulations. The new

Run	v_c [m/min]	a_p [mm]	σ_{vM} [MPa]	Proc. time [min]
10	272.00	24.00	202.84	1.30
11	281.00	24.00	208.07	1.26
12	259.00	24.50	204.43	1.37
13	289.00	25.00	205.04	1.23
14	296.00	25.00	217.38	1.20
15	300.00	25.00	202.62	1.18
16	300.00	26.00	206.87	1.19
17	298.00	27.00	205.52	1.20
18	298.00	28.00	205.23	1.20
19	300.00	29.00	209.47	1.20
20	255.00	14.50	294.47	2.51
21	255.00	16.50	246.26	1.95
22	165.00	29.50	279.08	2.18
23	169.00	29.50	288.69	2.12
24	106.00	30.00	387.52	3.39
25	116.00	30.00	356.80	3.10
26	129.00	30.00	344.63	2.78
27	134.00	30.00	342.61	2.68
28	154.00	30.00	325.50	2.33
29	284.00	30.00	219.06	1.27

TABLE 5. Case Study 2: Evaluation of selected predicted Pareto solutions. Iteration 1: solutions 10 to 19, Iteration 2: 20 to 29

Run	v_c [m/min]	a_p [mm]	σ_{VM} [MPa]	Proc. time [min]
15	300.00	25.00	202.62	1.18

TABLE 6. Case Study 2: Final Solution

incumbent Pareto solutions are solution 15. Then, the stooping criteria of the method are evaluated. Since one of the R^2 values for the metamodels is lower than 0.9900, then method continues iterating.

On the second iteration, the R^2 of the new models are 0.9995 and 1 for stress and process time respectively. The new predicted Pareto Solutions (20 to 29) are listed on Table 5. The incumbent Pareto Front was updated but no new Pareto solutions were identified. At this iteration the method stopped and the final Pareto Set and Front are reported on Table 6. On this application a unique solution that minimizes both objectives (stress and process time) was identified.

5. Conclusion

In summary, we presented the thermo-mechanic problem on a milling process and used a sequential surrogate based multiobjective simulation optimization method to solve two case studies of this machining process. The goal was to find the controllable process variables that optimize two performance measures of the milling process simultaneously. In general, the method was able to approximate a Pareto Front in a modest number of evaluations, which is critical for the cases of interest where a single simulation or experimental run can be costly and time consuming.

As future work, we will apply the optimization method to thermomechanical case studies with more than 2 PMs. Also, we will investigate how to account for process variability in the optimization method.

Acknowledgement

The authors gratefully acknowledge the financial support by the Mexican National Council for Science and Technology (CONACYT) and the German Academic Exchange Service (DAAD) through the project "Simulación Numérica y Optimización para Procesos Dependientes del Tiempo en Ingeniería y Ciencias de los Materiales". The second author also acknowledges the support given by the German Research Foundation (DFG) to the project "Thermomechanical Deformation of Complex Workpieces in Drilling and Milling Processes" within the DFG Priority Program 1480 "Modeling, Simulation and Compensation of Thermal Effects for Complex Machining Processes".

References

[1] R. R. Barton. Simulation optimization using metamodels. In *Winter Simulation Conference*, pages 230–238. Winter Simulation Conference, 2009.

[2] B. Denkena, P. Maaß, A. Schmidt, D. Niederwestberg, J. Vehmeyer, C. Niebuhr, and P. Gralla. *Modelling, Simulation and Compensation of Thermal Effects of Complex Machining Processes*, chapter Thermomechanical Deformation of Complex Workpieces in Milling and Drilling Processes. to appear in Springer-Verlag, 2017.

[3] B. Denkena, A. Schmidt, J. Henjes, D. Niederwestberg, and C. Niebuhr. Modeling a thermomechanical NC-simulation. *Procedia CIRP*, 8:69–74, 2013.

[4] B. Denkena, A. Schmidt, P. Maaß, D. Niederwestberg, C. Niebuhr, and J. Vehmeyer. Prediction of temperature induced shape deviations in dry milling. *Procedia CIRP*, 31:340–345, 2015.

[5] S. Dong, E. Chunsheng, B. Fan, K. Danai, and D. O. Kazmer. Process-driven input profiling for plastics processing. *Journal of Manufacturing Science and Engineering*, 129(4):802–809, 2007.

[6] S. W. Kok and R. Tapabrata. A framework for design optimization using surrogates. *Engineering Optimization*, 37(7):685–703, 2005.

[7] Y. F. Li, S. H. Ng, M. Xie, and T. N. Goh. A systematic comparison of metamodeling techniques for simulation optimization in decision support systems. *Applied Soft Computing*, 10(4):1257 – 1273, 2010.

[8] J. Montalvo-Urquizo, Z. Akbay, and A. Schmidt. Adaptive finite element models applied to the laser welding problem. *Computational Materials Science*, 46(1):245 – 254, 2009.

[9] J. Montalvo-Urquizo, P. Bobrov, A. Schmidt, and W. Wosniok. Elastic responses of texturized microscale materials using FEM simulations and stochastic material properties. *Mechanics of Materials*, 47:1 – 10, 2012.

[10] C. Niebuhr, D. Niederwestberg, and A. Schmidt. Finite element simulation of macroscopic machining processes-implementation of time dependent domain and boundary conditions. *Berichte aus der Technomathematik, Universität Bremen*, 14-01, 2014.

[11] A. Schmidt, E. Bänsch, M. Jahn, A. Luttmann, C. Niebuhr, and J. Vehmeyer. Optimization of engineering processes icluding heating and time-dependent domains. Springer IFIP AICT Series, 2016.

[12] A. Schmidt and C. Niebuhr. (ideas about) adaptive fem for problems with time-dependent domains. volume 42, pages 56–58. Oberwolfach Report, 2016.

[13] A. Schmidt and K.G. Siebert. *Design of Adaptive Finite Element Software: The Finite Element Toolbox ALBERTA*. Springer Heidelberg, 2005.

[14] T. W. Simpson, J. D. Poplinski, P. N. Koch, and J. K. Allen. Metamodels for computer-based engineering design: survey and recommendations. *Engineering with computers*, 17(2):129–150, 2001.

[15] G. T. Smith. *Cutting Tool Technology: Industrial Handbook*. Springer London, London, 2008.

[16] B. Suhr. *Simulation of steel quenching with interaction of classical plasticity and TRIP: numerical methods and model comparison*. Logos Verlag, 2010.

[17] H. Tschätsch and A. Reichelt. Milling. In *Applied Machining Technology*, pages 173–223. Springer Berlin Heidelberg, Berlin, Heidelberg, 2009.

[18] M. G. Villarreal-Marroquin, M. Cabrera-Rios, and J. M. Castro. A multicriteria simulation optimization method for injection molding. *Journal of Polymer Engineering*, 31(5):397–407, 2011.

[19] M. G. Villarreal-Marroquin, C. Po-Hsu, R. Mulyana, T. J. Santner, A. M. Dean, and J. M. Castro. Multiobjective optimization of injection molding using a calibrated predictor based on physical and simulated data. *Polymer Engineering & Science*, 2016.

[20] M. G. Villarreal-Marroqun, J. D. Svenson, F. Sun, T. J. Santner, A. M. Dean, and J. M. Castro. A comparison of two metamodel-based methodologies for multiple criteria simulation optimization using an injection molding case study. *Journal of Polymer Engineering*, 33(3):193–209, 2013.

[21] G. G. Wang and S. Shan. Review of metamodeling techniques in support of engineering design optimization. *Journal of Mechanical design*, 129(4):370–380, 2007.

[22] H. Zhou. *Computer modeling for injection molding: simulation, optimization, and control*. John Wiley & Sons, 2012.

Cátedras CONACYT, Centro de Investigación en Matemáticas, A.C., CIMAT-Monterrey, México
E-mail address: jonathan.montalvo@cimat.mx

University of Bremen, Center for Industrial Mathematics, Germany
E-mail address: niebuhr@math.uni-bremen.de

Cátedras CONACYT, Centro de Investigación en Matemáticas, A.C., CIMAT-Monterrey, México
E-mail address: maria.villarreal@cimat.mx